NAIC-ID(RS)T-0139-96

NATIONAL AIR INTELLIGENCE CENTER

SELECTED ARTICLES

**Approved for public release:
distribution unlimited**

DISCLAIMER NOTICE

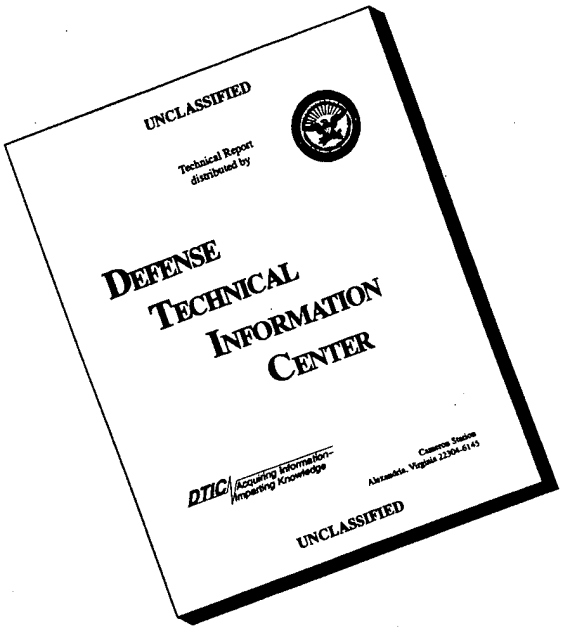

THIS DOCUMENT IS BEST QUALITY AVAILABLE. THE COPY FURNISHED TO DTIC CONTAINED A SIGNIFICANT NUMBER OF PAGES WHICH DO NOT REPRODUCE LEGIBLY.

HUMAN TRANSLATION

NAIC-ID(RS)T-0139-96 23 April 1996

MICROFICHE NR: 96C000350

SELECTED ARTICLES

English pages: 21

Source: Qiangjiguang Yu Lizishu (High Power Laser and Particle Beams), Vol. 1, Nr. 4, November 1989; pp. 319-329

Country of origin: China
Translated by: Leo Kanner Associates
F33657-88-D-2188
Requester: NAIC/TATD/Bruce Armstrong
Approved for public release: distribution unlimited.

TABLE OF CONTENTS

GRAPHICS DISCLAIMER

All figures, graphics, tables, equations, etc. merged into this translation were extracted from the best quality copy available.

Thermal Blooming of Collimated Pulsed High Power Laser Beams Propagating Upwards In the Atmosphere

Wang Yingjian and Gong Zhiben

(Anhui Institute of Optics and Fine Mechanics)

Abstract: Using the numerical simulation method and real atmospheric parameter modes, the effect of nonlinear thermal blooming on upward propagation of collimated pulsed high power laser beams in the atmosphere have been studied on the basis of the wave optics approach. The results show that such blooming, even though small, has critically bad effect on the laser beam front and its divergence.

Key Words: Propagation, Thermal Blooming

1. Introduction

The nonlinear thermal blooming effect on high power laser propagation upward through the atmosphere has become one of the crucial problems in intensive laser atmospheric propagation. Generally, atmospheric gas density decreases with height, which inevitably leads to reduction of atmospheric gas absorption coefficient with height. With this scenario, variation of absorption coefficient along the propagation distance that used to be ignored has to be taken into consideration in research on the nonlinear thermal blooming effect over high power laser slant atmospheric propagation [1].

2. Numerical Calculation Model and Calculation Parameters

The basic coupled equations describing the thermal blooming effect on high power laser atmospheric propagation [2] are: near-axis beam scalar wave equation

$$2ik\frac{\partial\varphi}{\partial z}+\nabla_T^2\varphi+k^2\left(\frac{n^2}{n_0^2}-1\right)\varphi=0 \tag{1}$$

acoustic wave equation

$$\left(\frac{\partial}{\partial t}+v_x\frac{\partial}{\partial x}\right)\left[\nabla^2-\frac{1}{c_s^2}\left(\frac{\partial}{\partial t}+v_x\frac{\partial}{\partial x}\right)^2\right]\sigma(r,z,t)=-\frac{(\gamma-1)}{\gamma p_0}\nabla^2\alpha(z)I(r,z,t) \tag{2}$$

Lorentz-Lorenz Law

$$n(r,z,t)=(n_0-1)\sigma(r,z,t) \tag{3}$$

where φ is optical field compound amplitude function; ∇^2 is Laplacian operator; $\alpha(z)$ is atmospheric gas absorption coefficient, i.e. absorption power density along unit length; $I(r,z,t)$ is light intensity, $I=|\varphi^2|$; σ is air compression ratio; k is number of waves; n is atmospheric refraction distribution after perturbance; n_0 is non-perturbated atmospheric refraction ratio; c_s is sound velocity; p_0 is atmospheric pressure intensity; $\gamma=c_p/c_v$, c_p and c_v respectively are constant pressure and constant volume specific heat; v_x is atmospheric transverse average wind speed. With the Fourier transformation, numerical calculation [3] is made over equation (1), and equation (2) is discussed under the following two approximations (numerical integration is calculated with the trapezoidal integration method) [2,3]

long pulse constant pressure approximation

$$\sigma(r,z,t)=-\frac{\gamma-1}{\gamma p_0}\alpha(z)\int_0^t I(r,z,t')\mathrm{d}t' \tag{4}$$

continuous laser stable thermal blooming

$$\sigma(r,z,t)=-\frac{\gamma-1}{\gamma p_0}\alpha(z)\int_{-\infty}^{x} I(x',y,z)\mathrm{d}x' \tag{5}$$

Proper selection of atmospheric mode is vitally important to numerical simulation method. Due to lack of related systematic data in China, we, referring to the U.S. standard atmospheric optical mode [4,5], approximately selected variation of

atmospheric gas absorption coefficient with height as:

$$\alpha(h)=\alpha_0\exp(-\alpha_1 h) \quad (0\leqslant h<12\text{km}) \tag{6}$$

$$\alpha(h)=\alpha_0 \quad (12\leqslant h<80\text{km}) \tag{7}$$

$$\alpha(h)=0 \quad (h>80\text{km}) \tag{8}$$

where α_0 is ground absorption coefficient; α_1 is absorption coefficient attenuation rate; $\alpha_0=\alpha_0\exp(-12\alpha_1)$. The atmospheric average wind speed mode is expressed in the following relations:

$$v_{X1}=1.0+h \quad (0\leqslant h<12\text{km}) \tag{9}$$

$$v_{X1}=19.0-0.5h \quad (12\leqslant h<27\text{km}) \tag{10}$$

$$v_{X1}=1.0+(4.5\ 73)(100.0-h) \quad (27\leqslant h<100\text{km}) \tag{11}$$

where $v_{x1}=v_x/v_{x0}.v_{x0}$ is ground average wind velocity; h is height.

The transmitting beam is a truncated Guassian beam in simulation computation, i.e. the light intensity distribution on transmission end surface is

$$\psi(r,0,0)=\begin{cases}\exp\left(-\dfrac{r^2}{2a_0^2}\right) & (r\leqslant a_0)\\ 0 & (r>a_0)\end{cases} \tag{12}$$

where a_0 is flare radius at I/e peak value power density; thus, transmission aperture D is two times of a_0. The real atmosphere is the ideal atmosphere.

Table 1. Simulation computation parameters

1 地面吸收系数(m^{-1})	0.5×10^{-7}	5 吸收系数衰减率(m^{-1})	0.5×10^{-7}
2 发射波长(μm)	1.0	发射孔径(m) 6	9.0
3 地面风速(m/s)	3.5	脉冲光束脉宽(ms) 7	27.3
4 光斑半径(m)	4.5	8 发射峰值功率密度(W/cm^2)	$10^{8}-10^{9}$

Key: 1. Ground absorption coefficient; 2. Transmission wavelength; 3. Ground wind velocity; 4. Flare radius; 5. Absorption coefficient attenuation rate; 6. Transmission aperture; 7. Pulsed beam pulse width; 8 Transmission peak value power density

3. Numerical Simulation Result

Fig. 1 shows variation of distorted flare intensity distribution with propagation distance z, caused by thermal blooming effect during upward atmospheric propagation of a long-pulse collimated high power laser. It can be seen from the figure that light intensity at z=100 km is less distorted while when z respectively reaches 500 and 1000 km, the light intensity is strongly distorted, leading to drastic reduction of peak value intensity and concave intensity at the center of flare. This is because near-field beam phase distortion can give rise to beam divergence. Specifically, as transmitting beam is Guassian beam and beam intensity reaches the maximum value at flare center and gradually decreases outward, beam divergence angle caused by thermal blooming effect appears uneven, i.e. it has a maximum value at the beam center and gradually diminishes toward the beam edge, which results in maximum light deflection at beam center to formulate the concave beam intensity at flare center as indicated in Fig. 1. We define the ratio between increase of flare radius containing 85% total transmission power $\Delta a(z)$ and transmission distance Δz as beam average divergence angle θ_{tb} .

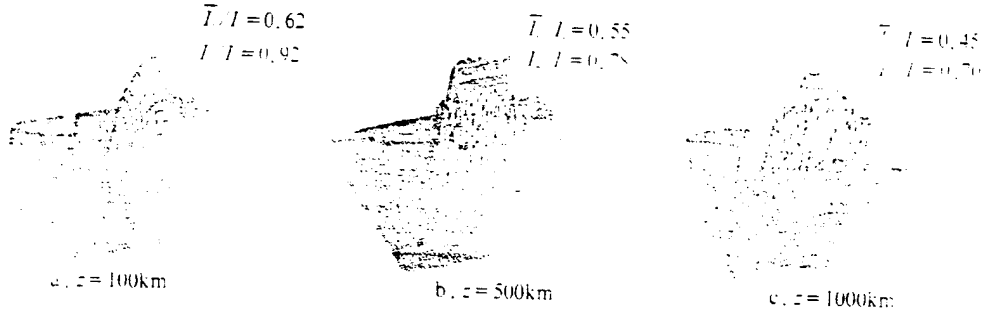

Fig. 1 Variation of distorted flare intensity distribution with Transmission Distance z(I_0 is transmission peak value power density; $I_0=10^6W/cm^2$; I_t is peak value power density; $\bar{I}_0$ is average power density on flare with a radius a_0; other parameters are the same as in Table 1).

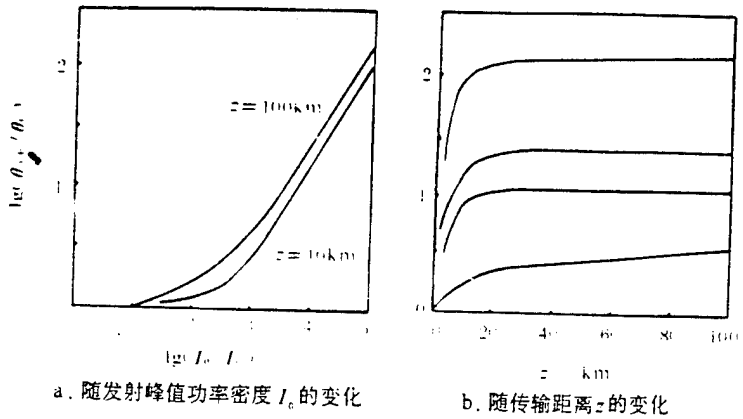

a. 随发射峰值功率密度 I_0 的变化　　b. 随传输距离 z 的变化

Fig. 2. Variation of beam divergence angle caused by thermal blooming (I_T=102W/cm2; the other parameters are the same as in Table 1)
a. Variation of power density I_c with transmission peak value
b. Variation of z with propagation distance

Fig. 2a and b show thermal blooming-initiated variation of ratio between θ_{tb} and diffraction angle θ_f with transmission peak value power density I_0 and z. From Fig.2a, when I_0 jumps to $10^4W/cm^2$, beam divergence angle has already greatly increased. I_0 can be defined, when beam divergence and flare distortion clearly

occur, as I_c, the threshold of peak value power density generating the thermal blooming effect. Under atmospheric parameters discussed in this paper, I_c is about $10^4 W/cm^2$, and once it reaches the thermal blooming threshold, the beam divergence angle will increase with increasing I_0 in approximate linearity. From Fig. 2b, since the atmospheric absorption coefficient appears very small over 20km in height and thermal blooming effect no longer takes place, the beam divergence angle will approach a constant. Within the range of laser power that interests us, the thermal blooming-initiated beam divergence angle is 1-2 orders larger than the diffraction angle.

Obviously, if the high power laser beam propagates upward with a particular dip angle, the thermal blooming-initiated beam divergence angle will rise even to a greater degree and the flare will distort even more dramatically as attenuation of atmospheric absorption coefficient with transmission distance becomes even slower at that time.

4. Conclusion

Even though the near-field thermal blooming effect seems rather weak during high power laser upward propagation in the atmosphere, it can cause beam phase distortion and its divergence angle to increase considerably, which can severely affect long-distance beam propagation and becomes a critical obstacle to high power laser atmospheric propagation. Hence, efficient methods are expected to be created to overcome the nonlinear thermal blooming effect.

References

[1] D.C.Smith, Proceedings of IEEE, 65(12), (1977).

[2] Gong Zhiben, Atmospheric Optics Proceedings, Anhui Institute of Fine Mechanics, Academia Sinica,(1976).

[3] J. Walsh and P.B. Virich, Topics in Appl. phys., 25, Chapter 7.

[4] R.A. Mcciatchey, AD-753075 (1970).

[5] D.E. Kelrip, Translated by Sun Jingwen, Wavelength Selection for Ground-based Free Electron Laser Device, China Research Academy of Physical Engineering.

Date of receiving paper: May 25, 1989

Date of receiving edited paper: August 22, 1989

Analysis of Factors Affecting Adaptive-Optics Correction of Turbulence

Shi Fang, Jiang Wenhan

(Institute of Optics and Electronics, Chinese Academy of Sciences, Chengdu)

Abstract: In this paper the criteria of the correction effect of an adaptive-optics turbulence correction system for laser transmission are discussed. By using the modulated transmission function (MTF) as the criterion, the relationships between the effects of turbulence correction by the adaptive-optics system and the parameters of the laser transmission system and atmospheric turbulence are analyzed by computer simulation.

Key Words: Adaptive optics, atmospheric turbulence, laser transmission system, modulated transmission function (MTF)

1. Introduction

When a laser beam propagating through the atmosphere arrives at the target, its flares may diffuse and its energy concentration may decrease as a result of the influence of atmospheric turbulence. In this circumstance, through real-time measurement and correction of the wavefront phase distortion brought about by atmospheric turbulence, the adaptive-optics phase compensation technique can be used to improve the quality of the laser beam propagating through the atmosphere.

Technically, it is of great significance in both theory and practice to make a theoretical quantitative analysis of the adaptive optics turbulence correction effect of the laser transmission system as well as to evaluate of the contribution of this technique and its basic limitations. A quantitative analysis of the turbulence correction effect of a laser

transmission system involves two aspects: (1) which criterion is used to assess the turbulence correction effect and (2) the relationship between the correction effect, laser transmission system parameters, adaptive-optics system parameters, and atmospheric turbulence parameters.

Through analysis and comparison, this paper provides the optical modulated transmission function of the general system, i.e. the optical modulated transmission function of all optical channels including the turbulent atmosphere system, the laser transmission system and the adaptive-optics system as the criterion for the turbulence correction effect. In addition, we constructed the theoretical relationship and a computer model of atmospheric turbulence adaptive-optics correction in accordance with atmospheric turbulence theory and also, through computer calculations, produced some of the relationship curves between the criteria, the laser transmission adaptive system and atmospheric turbulence parameters, which formed the theoretical and quantitative basis for further research.

2. Criteria for Correction Effect

Upon arriving at the target after atmospheric propagation, a laser beam suffers from a decrease in quality under the effect of atmospheric turbulence. So the technique of adaptive optics, performing real-time compensation for stochastic phase errors brought about by atmospheric turbulence, can improve laser beam quality. In this case, how to use a quantitative criterion to determine beam quality deterioration due to turbulence, as well as how to assess improvement of beam quality following adaptive optical correction, becomes a critical problem to be solved in practical development of the laser transmission adaptive-optics system, its theoretical analysis and computer simulation.

A criterion that can be used to evaluate the atmospheric

turbulence correction effect should meet the following requirements: (1) The criterion must reflect the stochastic phase error of atmospheric turbulence and must be in monotonic variation with turbulence intensity; (2) the criterion must have accurate physical implications and be realized through practicable measurement; (3) for theoretical and numerical analysis, the criterion must form clear, analytical or numerical relations with the major parameters of the laser transmission system, atmospheric turbulence parameters and adaptive-optics correction system parameters.

At present, there are many criteria adopted to assess the atmospheric turbulence correction effect of an adaptive-optics system, including:

(1) Strior ratio [1]

$$R_S = \frac{I}{I_0} \tag{1a}$$

Given a small image error

$$R_S = \frac{I}{I_0} = e^{-\sigma^2} \tag{1b}$$

where I and I_0, respectively are central light intensity with turbulence-initiated phase distortion and central light intensity in an ideal system; σ^2 is the wavefront mean square error.

(2) Flare size d_0 [2]

$$e^{-1} = E_0^{-1} \int_0^{2\pi} d\theta \int_0^{d_0/2} I(r)\, r\, dr \tag{2}$$

where d_0 is the equivalent diameter of the integration region when the ratio between flare energy on the target and total light energy arriving at the target is e^{-1}; I(r) is light intensity distribution on target.

(3) Energy concentration

$$E(r_E) = \iint d^2 r\, I(r) \qquad (|r| < r_E) \tag{3}$$

i.e. radius at target center is the integration energy in the r_E region. It can be seen that criteria (2) and (3) are in a direct correspondence relation.

(4) Optical modulated transmission function of general system (MTF) [3]

$$\langle \tau(l) \rangle = \int \langle G(r+\frac{l}{2}) G^*(r-\frac{l}{2}) \rangle W(r+\frac{l}{2}) W^*(r-\frac{l}{2}) d^2 r \tag{4}$$

where < > means system-averaged; <G(r+l/2)G*(r-l/2) is the perturbation contribution (l is distance vector between any two points on the pupil surface; r is pupil surface coordinate). MTF is the system-averaged conjugated phase on the surface of the pupil, which is created by the atmospheric turbulence stochastic phase distortion, the transmission system optical phase error and the adaptive-optics correction. It contains three parts: atmosphere, transmission system and adaptive-optics system, and is therefore referred to as the optically modulated transmission function of the general system; W(r) is pupil function; collimated plane wave with a transmission aperture D is as follows:

$$W(r) = \begin{cases} 1, & |r| \leq D/2 \\ 0, & |r| > D/2 \end{cases} \tag{5}$$

Analysis and comparison of the foregoing criteria show that they all increase with decreasing phase error and reach a maximum value when the image error is equal to zero. While MTF has its own unique advantages, such as ability to directly reflect the stochastic phase error of atmospheric turbulence; its expression is appropriate for both large and small image errors and also reflects the relationship between adaptive-optics model image error correction terms. In addition, based on MTF, the foregoing criteria can be associated with one another. For isotropic atmospheric turbulence conforming to the Kolmogrov spectrum

$$R_S = \frac{\int l\,\mathrm{d}l\langle\tau(l)\rangle}{\int l\,\mathrm{d}l\,\tau_0(l)} \tag{6}$$

$$e^{-1} = \frac{\int_0^{d_0/2}\mathrm{d}r\int_0^{1} J_0(2\alpha l)\langle\tau(l)\rangle l\,\mathrm{d}l}{\int_0^{\alpha}\mathrm{d}r\int_0^{1} J_0(2\alpha l)\tau_0(l)\,l\,\mathrm{d}l} \tag{7}$$

where J_0 is zero-order Bessel function; α=kDP/2z is normalized radius of the receiving surface, k=2π/λ is number of waves; λ is wavelength; λ is wavelength; P is upper radius of receiving surface; z is transmission distance.

$$E(r_E) = N_F^2\int_0^{r_E}\mathrm{d}r\int_0^{1} J_0(2\alpha l)\langle\tau(l)\rangle l\,\mathrm{d}l \tag{8}$$

where N_F is Feiner number.

Obviously, the MTF of the overall system can not only more accurately reflect the influence of atmospheric turbulence and adaptive-optics mode correction, but also be used for theoretical analysis and numerical calculation. Therefore, it is a desirable criterion for evaluating the turbulence correction effect of laser transmission systems.

3. Calculation Model

Based on their isotropic character, the perturbation term in equation (4) and turbulent atmosphere-initiated stochastic wave surface error can be expressed as follows [5]:

$$\langle G(r+\frac{l}{2})G^{*}(r-\frac{l}{2})\rangle=\langle\exp\{[A(r+\frac{l}{2})+i\psi(r+\frac{l}{2})]+$$
$$[A(r-\frac{l}{2})+i\psi(r-\frac{l}{2})]\}\rangle=\exp[-\frac{D(l)}{2}] \quad (9)$$

where A(r) and ψ(r) are logarithmic amplitude and phase perturbation of turbulence; D(l) is the wave surface structure function, which can be calculated, in the case of Kolmogrov type turbulent atmosphere, as:

$$D(l)=6.88(\frac{l}{r_0})^{5/3}$$

where r_0 is turbulence coherent length expressing its intensity

$$r_0=[0.423k^2\int_0^z C_n^2(h)dh]^{-3/5} \quad (10)$$

where C_n^2 is atmospheric refraction ratio structure constant; z is transmission distance; $k=2\pi/\lambda$, λ is wavelength.

Atmospheric turbulence-initiated phase perturbation ψ(r) can be expressed with the sum of a series of model image errors [6] as follows:

$$\psi(r)=\sum_i a_i F_i(r) \quad (11)$$

where F_i(r) is i model image error function; a_i is its corresponding coefficient, a function of time t. We selected simple Zernike polynomial as the model image error function[7] as follows:

$$F_i(r)=\sqrt{2(n+1)}\,R_n^m(r)\cos m\theta \quad (i \text{ is an even number}, m\neq 0)$$
$$F_i(r)=\sqrt{2(n+1)}\,R_n^m(r)\sin m\theta \quad (i \text{ is an odd number}, m\neq 0)$$
$$F_i(r)=\sqrt{n+1}\,R_n^0(r) \quad (m=0) \quad (12)$$

where $R_n^m(r)$ is radial function

$$R_n^m(r)=\sum_{s=0}^{(n-m)/2}\frac{(-1)^s(n-s)!}{s![(n+m)/2-s]![(n-m)/2-s]!}(\frac{2r}{D})^{n-2s} \quad (13)$$

where D is transmission optical system aperture; n is radial order; m is angular order; they are in the relation

=even number; the relationship between i, n and m can be deduced from Zernike polynomial [7].

The polynomial exhibits orthogonality in the circular region:

$$\int d^2 r W'(r) F_i(r) F_{i'}(r) = \pi D^2 \delta_{ii'} \tag{14}$$

Thus, with orthogonality, the model coefficient in equation (11) can be derived as follows:

$$a_i = \int d^2 r W'(r) \psi(r) F_i(r) \tag{15}$$

An adaptive-optics system performs correction in two steps: first, detection of phase perturbation $\psi(r)$ brought about by atmospheric turbulence; secondly, compensation of the phase error of atmospheric turbulence in advance with the conjugated model image error on the transmission system pupil surface by using a deformation mirror. However, with a limited number of detecting subapertures of the adaptive-optics system and the drivers of the deformation mirror, the system can correct only a limited number of model image errors. In the case when the adaptive optics system can correct the first N image errors, then the compensation phase can be obtained as follows:

$$\varphi(r) = \sum_{i=2}^{N} a_i F_i(r) \tag{16}$$

while the remaining image errors after correction will be:

$$\delta(r) = \psi(r) - \varphi(r) = \sum_{i=2}^{\infty} a_i F_i(r) - \sum_{i=2}^{N} a_i F_i(r) \tag{17}$$

Substituting this result into equation (4) and neglecting the image errors of the transmission system itself, the MTF corrected by adaptive-optics system can be expressed as follows:

$$\langle \tau(e) \rangle = 4D^2 \exp\left[-\frac{1}{2} D(l) \int_0^{\pi/2} d\theta \int_0^{L(\theta)} r dr \exp\{ \frac{1}{2} Q(l, r) \right. \tag{18}$$

$$\left. + \sum_{i=2}^{\infty} \sum_{i=i-1}^{i_{max}} \langle a_i a_{i'} \rangle [F_i(r + \frac{l}{2}) - F_i(r - \frac{l}{2})][F_{i'}(r + \frac{l}{2}) - F_{i'}(r - \frac{l}{2})] \right\}$$

where

$$L(\theta) = -\frac{l}{2} \cos(\theta - \varphi) + \frac{l}{2} \left[\left(\frac{l}{D} \right)^{-2} - \sin^2(\theta - \varphi) \right]^{1/2} \tag{19}$$

θ and φ respectively are angles of vectors r and l, while

$$Q(l, r) = \sum_{i=2}^{\infty} \sum_{i=2}^{\infty} \langle a_i a_{i'} \rangle [F_i(r + \frac{l}{2}) - F_i(r - \frac{l}{2})][F_{i'}(r + \frac{l}{2}) - F_{i'}(r - \frac{l}{2})] \tag{20}$$

$\langle a_i\ a_i \rangle$ is the relationship between i model and i model coefficient, which can be calculated from the turbulence wave surface structure function D(l) [9] as follows:

$$\langle a_i a_{i'} \rangle = \begin{cases} 0.0072 (D/r_0)^{5/3} (-1)^{(n+n'-2m)/2} [(n+1)(n'+1)]^{1/2} \pi^{8/3} \delta_{mm'} \\ \dfrac{\Gamma(\frac{14}{3}) \Gamma[(n+n'-\frac{5}{3})/2]}{\Gamma[(n-n'+\frac{17}{3})/2] \Gamma[(n'-n+\frac{17}{3})/2] \Gamma[(n+n'+\frac{23}{3})/2]} \cdot & (i\text{-}i' \text{ is even number}) \\ 0, \quad (i-i' \text{为奇数}) & \end{cases} \tag{21}$$

(i-i′ is odd number)

where Γ is Gamma function. $i_{max} \to \chi_c$ can be theoretically established in equation (18). Nevertheless, with increase in i-i′, the relationship between individual models the coefficients in turbulence rapidly decreases. In this case, i_{max} can be truncated in calculations when it is large enough, but this can by no means affect calculation precision.

According to equation (18), overall system MTF can be calculated after N image errors have been corrected, which, compared with MTF without correction, exhibits the effect and contribution of the adaptive-optics correction. In addition, (18) and other equations also show the relationship between the

overall system MTF and various atmospheric conditions including refraction structure constant C_n^2, atmospheric coherent length r_0, laser transmission system aperture D, wavelength λ and transmission distance z. After establishing the theoretical model of the relationship between atmospheric turbulence and the adaptive-optics correction, we worked out calculation procedures and conducted simulation computations.

4. Computer Simulation Result

Based on the foregoing theoretical model, computer simulation was made of adaptive corrections under different turbulence conditions in five wavelengths and as a result, the overall system MTF curves corresponding to these parameters were plotted. In addition, MTF without the adaptive-optics system correction and the MTF curves under ideal conditions (with no effect from atmospheric turbulence) were also presented for comparison. The ordinates in the figures represent normalized MTF values, while the abscissae show the normalized spatial frequencies, with the spatial cutoff frequency of the system being 1.0. Also, these figures indicate the number of N image error models corrected by individual curves, along with wavelengths (unit: μm). Fig. 1-3 shows the laser overall system MTF curves at the wavelength 0.6238 μm: the bottom curve stands for the uncorrected MTF curve, while the uppermost one stands for the MTF curve of an ideal system. With an increase in the number of corrected terms, the curves rise alternatively. Fig. 4-5 shows the overall system MTF curves at 1.0 μm, while other parameters are the same as in Fig. 1-3. These calculated curves suggest that:

(1) with the increasing turbulence intensity (i.e. increase in D/r_0), the overall-system MTF rapidly decreases, and as does the spatial cutoff frequency.

(2) Under the same conditions of turbulence, atmospheric turbulence affects long wavelength light more than short wavelength light because r_0 and wavelength form a 6/5 square.

(3) With increased in N, which is the number of models corrected by the adaptive-optics system, the overall-system MTF increases, thereby improving of the system.

(4) When the effect of turbulence is smaller ($D/r_0=2$), the overall-system MTF can be greatly improved, approaching the ideal value with only a few models to be corrected, and furthermore, better improvement occurs in low-order terms. On the other hand, when the turbulence effect appears larger ($D/r_0=10$), the same degree of improvement requires a correction over more image-error models, and better MTF improvement concentrates on high-order terms.

(5) Once the number of image error orders reaches a particular value, increasing the number of correction terms will no longer help in improving the MTF curve. In this case, improving the MTF curve is possible only at the cost of much higher complexity of adaptive-optics system.

(6) Since the correction capability of the adaptive-optics system is limited to image errors in finite terms, the overall system MTF after correction of finite terms cannot reach the ideal value in any case, particularly when turbulence has a stronger effect.

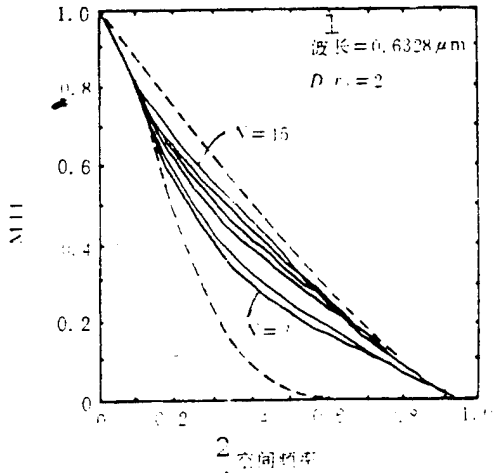

Fig. 1 MTF with λ =0.6328μm and D/r_0=2 (solid lines are respectively N=3,4,6,8,10,15 from bottom up; upper imaginary line represents diffraction limit while lower imaginary line--MTF without correction)

Key: 1. Wavelength 2. Spatial frequency

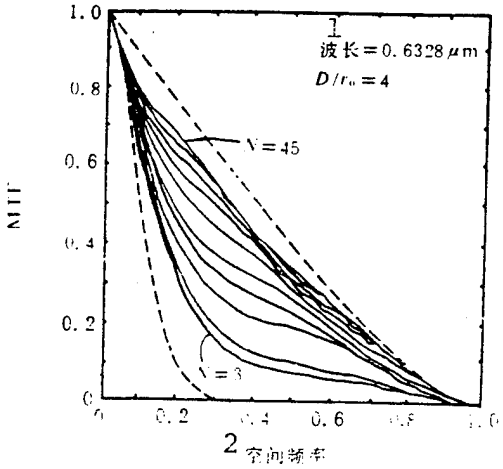

Fig. 2 MTF with λ=0.6328μm and D/r_0=4(solid lines respectively are N=3,4,6,8,10,15,21,28,36,45 from bottom up; upper imaginary line stands for diffraction limit while lower imaginary line--MTF without correction)

1 Wavelength; 2. Spatial frequency

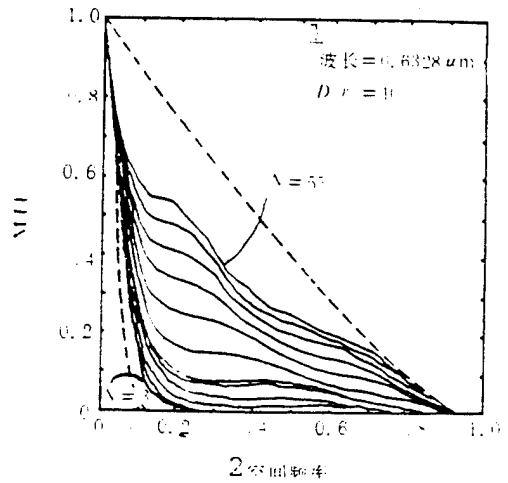

Fig. 3 MTF with λ =0.6328μm and D/r_0=10(solid lines respectively are N=3,4,6,8,10,11,15,21,28,36,45,55 from bottom up; upper imaginary line represents diffraction limit while lower imaginary line--MTF without correction)

Key: 1. Wavelength; 2. Spatial frequency

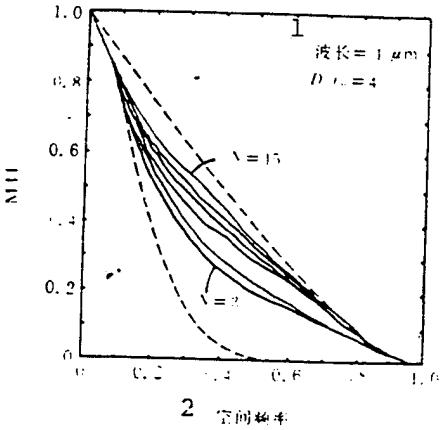

Fig. 4 MTF with λ =1μm and D/r_0=4(solid lines respectively are N=3,4,6,8,10,15 from bottom up; upper imaginary line represents diffraction limit while lower imaginary line--MTF without correction)

Key: 1 Wavelength; 2. Spatial frequency

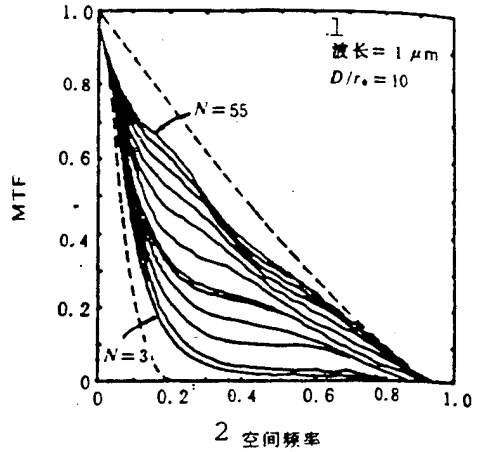

Fig. 5 MTF with λ=1μm and D/r_0=10 (N of individual curves corresponds to that in Fig. 3; upper imaginary line stands for diffraction limit while lower imaginary line--MTF without correction)

Key: 1. Wavelength; 2. Spatial frequency

5. Conclusion

With the modulated transmission function of the overall system as a fundamental criterion and based on atmospheric turbulence theory, a calculation model of adaptive-optics atmospheric turbulence correction was established in this paper. Computer simulation results exhibited the effect of the adaptive-optics system correction over atmospheric turbulence and proved that this system is efficient in improving overall system MTF, i.e. it can greatly raise the beam quality of the laser transmission system through correction over a limited number of image error models. However, as far as a large aperture laser transmission system is concerned, it is required to correct an increasing number of image errors due to strong effect from turbulent perturbation. Therefore, the complexity of the adaptive-optics system depends on atmospheric turbulence conditions as well as the laser transmission aperture. In addition, in view of adaptive optics, long wavelength laser

transmission is found to be preferable.

References

[1] Fritz Merkle. "Mirror developments for adaptive optics". LEST foundation technique report. No.28(1988)

[2] J.Y.Wang. Appl. Opt., 17 (16), 2580 (1978).

[3] J.Y.Wang. J. Opt.Soc.. Am., 68 (1). 78 (1978).

[4] Ibid. 67 (3), 383 (1978).

[5] D.L. Fried, ibid. 56 (10). 1372 (1966).

[6] U. Bonn, E. Wolf, Optics Principle (Vol. 2), Science Press.

[7] Robert V. Noll, J. Opt. Soc. Am., 66(3), 207(1976)

This paper was received for publication on July 18, 1989.

The revised paper was received on September 4, 1989.

DISTRIBUTION LIST

DISTRIBUTION DIRECT TO RECIPIENT

ORGANIZATION	MICROFICHE
B085 DIA/RTS-2FI	1
C509 BALL0C509 BALLISTIC RES LAB	1
C510 R&T LABS/AVEADCOM	1
C513 ARRADCOM	1
C535 AVRADCOM/TSARCOM	1
C539 TRASANA	1
Q592 FSTC	4
Q619 MSIC REDSTONE	1
Q008 NTIC	1
Q043 AFMIC-IS	1
E404 AEDC/DOF	1
E410 AFDTC/IN	1
E429 SD/IND	1
P005 DOE/ISA/DDI	1
1051 AFIT/LDE	1
PO90 NSA/CDB	1

Microfiche Nbr: FTD96C000350
NAIC-ID(RS)T-0139-96